Results in Materials 19 (2023) 100441

Contents lists available at ScienceDirect

Results in Materials

journal homepage: www.sciencedirect.com/journal/results-in-materials

# Dynamic characteristics of cracked simply supported bidirectional functionally graded Rayleigh beam

Talib EH. Elaikh [a], Nada M. Abd [a], Ali Hasan Ali [b,c,d,*]

[a] Department of Mechanical Engineering, University of Thi-Qar, Nassiriya, 64001, Iraq
[b] Institute of Mathematics, University of Debrecen, Pf. 400, H-4002, Debrecen, Hungary
[c] Department of Mathematics, College of Education for Pure Sciences, University of Basrah, Basrah, 61001, Iraq
[d] College of Engineering Technology, National University of Science and Technology, Dhi Qar, 64001, Iraq

ARTICLE INFO

*Keywords:*
Bidirectional FGM beam
Rayleigh beam theory
Open crack
Galerkin's technique

ABSTRACT

This paper investigates the dynamic behavior of cracked Rayleigh beams constructed from bidirectional functionally graded (BDFG) materials under simple boundary conditions. A torsional massless spring is employed to model the beam's open crack type. The vibration equations are obtained using Hamilton's principle. The graded beam material properties are varied throughout the thickness based on the power-law distribution and in the longitudinal direction using the exponential material distribution. To solve the dynamic equations, Galerkin's approach is employed. The paper evaluates the impacts of the axial index, gradient property index, beam modulus ratio, and crack parameters on the natural frequencies of the FG beam. The results indicate that the dimensionless natural frequencies of intact graded beams decrease with increased gradient index $k$. In contrast, they increase with a rise in the modulus ratio. Additionally, the results demonstrate that an increase in the crack depth ratio decreases dimensionless natural frequencies.

## 1. Introduction

Graded beam structures are widely used in various industries today, such as aircraft wings, satellites, docks, steel bridges, sea platforms, helicopter rotor blades, ships, buildings, offshore structures, spacecraft, and antennas. In the design of these structures, the vibration behavior of the beams is a crucial factor and has therefore received much attention in recent years [1–3]. The properties of materials that change in the thickness direction have also been extensively studied in recent years [4–6]. Several studies have investigated the vibration behavior of graded beams. In particular [7], developed vibration equations for graded beam shear and Euler models, which were solved using the Navier method [8]. studied the vibration behavior of a Timoshenko beam with graded material under axial compression, finding that increasing the beam core thickness resulted in an increase in the first three natural frequencies [9]. employed differential transformations (DT) to determine the natural frequencies of a graded beam connected to linear and torsional springs. The study found that the natural frequencies decreased as the volume fraction indexes increased [10]. investigated the vibration analysis of a Euler-graded beam model with shear deformation. The results showed that both gradient properties and shear deformation had a detrimental effect on the natural frequencies [11]. examined the vibration response of composite beams under a harmonic load. Shear deformation was considered, and the governing equations were derived using the Lagrange procedure. The numerical results were obtained using the Ritz method [12]. used the transfer matrix approach to study the natural frequencies of Euler and Timoshenko graded beams with different end supports, finding that the dimensionless frequencies decreased as the volume fraction index increased [13]. used finite element analysis to study the vibrations of a graded Timoshenko beam under various load conditions, and [14] derived the equations of free vibration for a graded beam with power law variation of properties through the thickness. In both cases, it was found that the gradient property index had a positive effect on the natural frequencies [15]. introduced an innovative Timoshenko microbeam model combined with a modified strain gradient theory. The study comprehensively investigated the static bending and buckling behaviors of microbeams embedded. By utilizing Navier solutions, the deflections of the beam and buckling loads were determined [16]. used dynamic stiffness to find the vibration frequencies of a graded beam and found that the power-law exponent decreased as the power-law exponent increased. The impact of transverse loading on 3D-printed FG beams and

* Corresponding author. Institute of Mathematics, University of Debrecen, Pf. 400, H-4002, Debrecen, Hungary.
*E-mail addresses:* lecturetalib@gmail.com (T.EH. Elaikh), mech.eng.nada94@utq.edu.iq (N.M. Abd), ali.hasan@science.unideb.hu (A.H. Ali).

https://doi.org/10.1016/j.rinma.2023.100441
Received 16 July 2023; Received in revised form 14 August 2023; Accepted 18 August 2023
Available online 22 August 2023

functionally graded sandwich (FGS) beams was investigated through a combination of experimental and finite element analysis by Ref. [17]. When comparing 3D-printed FGS beams with non-graded foam, it was observed that the former exhibited greater strength [18]. analyzed the free vibration and buckling of a graded beam using various beam theorems and found that the fundamental frequencies increased as the power-law and porosity indices decreased.

Most research on functionally graded materials (FGMs) has primarily focused on the variation of material properties in one direction (1D), with fewer studies examining graduated beams in two directions (2D). In Ref. [19], the material properties of a graded Timoshenko beam were assumed to vary in both the axial and thickness directions according to the power law. The Ritz approach was used to analyze the buckling of this beam, and the effects of the buckling load, shear deformation factor, and various end supports on the natural frequencies were obtained. Similarly [20], studied the free vibration of a graded Euler beam that followed the power law in both the axial and thickness directions. These studies demonstrate the potential for using FGMs in beam structures and the importance of considering the directionality of these materials in design and analysis. However, more research is needed to fully understand the behavior of 2D graduated beams and their potential applications. The influence of axial force varies with time on the vibration response of (BDFG) beams was explored by Ref. [21]. To formulate the nonlinear vibration equation, Timoshenko beam theory, along with Hamilton's principle, was utilized. The continuous model was discretized using the Galerkin scheme.

Additionally, cracks play a significant role in the failure of a wide range of engineering structures. The presence of cracks in the geometric design reduces the rigidity of the structure, thereby affecting its vibration characteristics [22,23]. The vibration characteristics are impacted by multiple factors, such as the crack depth, position within the structure, and the number of cracks [24]. Therefore, many researchers have studied the effect of cracks in homogenous and graded structures [25]. demonstrated the effect of cracking on a homogeneous beam. The motion equations were formulated using different beam models and then solved using the Galerkin method [26]. conducted a vibration analysis of cantilever small-size Euler beams with edge-cracked utilizing the (MCST) and the finite element method. The material properties of the beam were considered to exhibit an exponential distribution along the height direction. A massless elastic rotational spring was introduced to simulate the presence of a crack in the beam [27]. studied the inverse and direct vibrations of a cracked beam with pinned-pinned ends using a massless rotational spring with syllabic flexibility to model the crack. The eigenvalue, position of the crack, and its syllabic flexibility were all factors that influenced the characteristic equation. The validity of the theoretical findings was verified through comparison with experimental results. A vibration analysis of functionally graded (FG) nanobeam with an edge crack under transverse loading was studied by Ref. [28]. By combining the (MCST) and (EBT), vibration equations for cantilever beams were derived. Furthermore [29], explored the vibration behavior of a graded Euler cracked beam subjected to the impact of a longitudinal moving load and axial compressive load. The volume fraction variation of a graded material was expressed exponentially along with the beam thickness. The vibration equations were analyzed using a series expansion modal. The results indicated that a higher modulus of elasticity ratio leads to a smaller dynamic deflection of the beam [30]. focused on analyzing the elastic deflections of edge-cracked FG nanobeams subjected to transverse loading. The investigation employed the finite element method with the (MCST) and (EBT). These methodologies were employed to derive the bending equation for the nanobeams. In Ref. [31], investigators analyzed the free vibration of a graded Timoshenko beam that experienced multiple cracks. Hamilton's extended principle was utilized to derive the kinematic equations for the system, and the dynamic stiffness method was employed to solve the vibration equations and obtain the natural frequencies. The outcome demonstrated that the natural frequencies declined as the crack depth ratio and the number of cracks increased [32]. developed the vibration equations for a graded Timoshenko sandwich beam with cracks using a stiffness matrix approach. They found that increasing the depth of the crack reduces the frequency response values. In Ref. [33], the coercive vibration behavior of a graded micro-beam with a crack was investigated using two stress model while considering the damping effect. The Kelvin-Voigt model was employed to examine the damping effect [34]. investigated the vibration characteristics of an edge-cracked functionally graded cantilever Euler beam. Hamilton's principle was used to determine the differential equations of motion. In this study, a FEM was used to solve the problem. The properties of beam material vary exponentially with thickness beams [35]. investigated the multi-cracked graded Timoshenko beam, with cracks modeled as rotational springs. The results showed that the growth in the number and depth of the cracks causes a reduction in the natural frequencies. The free vibration of a graded Rayleigh moving beam with an open-type crack was investigated by Ref. [36].To achieve this, Hamilton's extended principle was used to derive the kinematic equations for the system. Galerkin's method was then utilized to solve the system equations and determine the natural frequencies associated with the system. This approach allowed us to understand better the free vibration of the graded Rayleigh moving beam and the effect of the open-type crack on the system. In a recent study [37], explored the effect of Mass per Unit Length on the natural frequency of a Rayleigh beam using the differential transformation method (DTM). The study found that increasing the Mass per Unit Length of the beam caused the natural frequency to decrease and vice versa. The results from the study showed that the DTM was an effective method for calculating the natural frequency of a Rayleigh beam, as it was able to approximate the exact solutions closely. The wave propagation of a cracked cantilever functionally graded (FG) beam was investigated by Ref. [38]. The system equation was deduced through the utilization of Lagrange's equations. Triangular impulses were employed to stimulate the beam.

As far as the authors are aware, there has been no report on the dynamic characteristics of two-dimensional functionally graded Rayleigh beams with cracks. Furthermore, the effects of 2-D graded materials, crack parameters, Rayleigh parameters, and the effective material ratio on the dynamical behavior have not been examined. Addressing this gap, the present investigation aims to investigate the vibration characteristics of supported Rayleigh beams constructed from bidirectional functionally graded materials with cracks. We present the mathematical model for the considered system, and derive the vibrational equations that incorporate the crack effects using Hamilton's principle. We introduce the solution methodology as well. To simulate the cracks, a massless torsional spring is utilized. We carry out our analysis using MATLAB software, which enables us to study how various parameters affect the vibration response.

## 2. Mathematical formulation

Consider the cracked bidirectional functionally graded (BDFG) Rayleigh beam illustrated in Fig. 1. The symbols $\alpha, x_c, L, b,$ and $h$ respectively denote the crack depth, crack location, beam length, beam width, and beam height. The upper edge of the beam consists of a material with a high ceramic content, while the lower edge comprises a material with a high metal content.

The modulus of elasticity and density in a two-dimensional direction is given as [39]

$$\left.\begin{aligned} E(x,z) &= f_1(x)\left((E_c - E_m)\left(\frac{z}{h}+\frac{1}{2}\right)^k + E_m\right) \\ \rho(x,z) &= f_2(x)\left((\rho_c - \rho_m)\left(\frac{z}{h}+\frac{1}{2}\right)^k + \rho_m\right) \end{aligned}\right\}, \tag{1}$$

in which $E_c$ and $E_m$ are the modulus of elasticity of ceramics and metals,

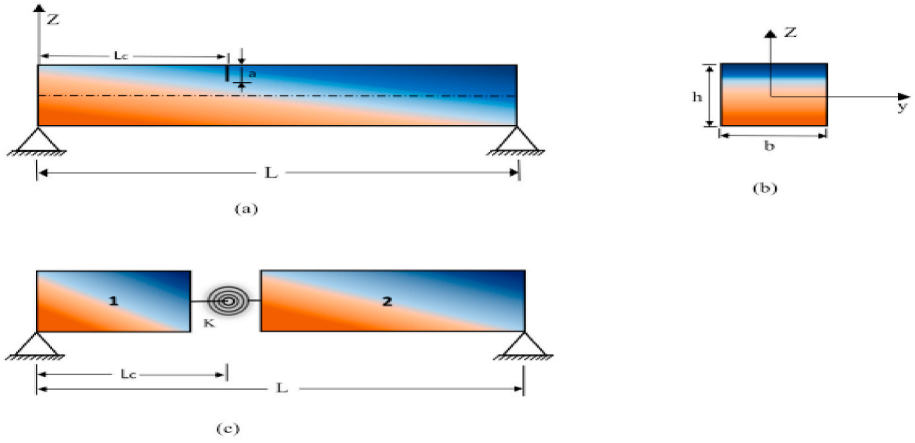


**Fig. 1.** Scheme diagram of (a) cracked FGM beam, (b) cross-section, (c) crack modeling as a rotational spring..

respectively. And respectively, $\rho_c$ and $\rho_m$ are the density of ceramics and metals. In the $x$ direction, the material properties vary according to the exponential function

$$f_1(x) = f_2(x) = e^{\beta \frac{x}{L}} \tag{2}$$

where $\beta$ represents the axial FG index. Figs 2 and 3 depict the changes in elasticity modulus for BDFG microbeams in the thickness and axial directions, respectively, which follow the same trends as the mass density distribution. These figures illustrate that distinct bi-directional FG indexes can result in different materials (see Fig. 4).

Based on Rayleigh's theory, the rotating inertia effect is taken into account, and the strain and stress equations of a functionally graded (FG) Rayleigh beam can be written as [40].

$$\left.\begin{aligned} \varepsilon_x &= \frac{\partial \overline{u}(x,t)}{\partial x} = -(z)\frac{\partial \varpi}{\partial x} = -z\frac{\partial^2 w}{\partial x^2} \\ \sigma_x &= \varepsilon_x E(x,z) = -zE(x,z)\frac{\partial^2 w}{\partial x^2} \end{aligned}\right\} \tag{3}$$

For cracked beam, the beam is split into two segments as shown in Fig. 1c. The potential energy $(P_E)$ of a cracked bi-directional graded Rayleigh beam is written as:

$$P_E = \frac{1}{2}\int_0^{x_c}\int_A \sigma_x \varepsilon_x dA dx + \frac{1}{2}\int_{x_c}^{L}\int_A \sigma_x \varepsilon_x dA dx = \frac{1}{2}\int_0^{x_c}\int_A E(x,z)\left(\frac{\partial^2 w_1}{\partial x^2}\right)^2 dA dx + \frac{1}{2}\int_{x_c}^{L}\int_A E(x,z)\left(\frac{\partial^2 w_2}{\partial x^2}\right)^2 dA dx \tag{4}$$

and, the kinetic energy of bi-directional FG Rayleigh beam with cracks is

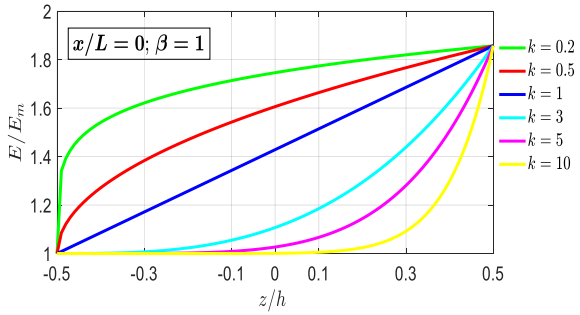


**Fig. 2.** Variation of elastic modulus ratio for bi-directional FG as a function of $z/h$.

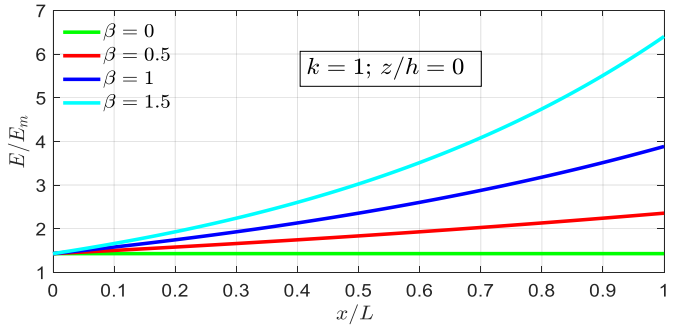


**Fig. 3.** Variation of elastic modulus ratio for BDFG with respect to $x/L$ Governing equation.

given as:

$$K_E = \int_0^{x_c}\left(\rho(x,z)A\left(\frac{\partial w_1}{\partial t}\right)^2 + \rho(x,z)I\left(\frac{\partial^2 w_1}{\partial x \partial t}\right)^2\right)dx + \frac{1}{2}\int_{x_c}^{L}\left(\rho(x,z)A\left(\frac{\partial w_2}{\partial t}\right)^2 + \rho(x,z)I\left(\frac{\partial^2 w_2}{\partial x \partial t}\right)^2\right)dx \tag{5}$$

To obtain the motion's equation, Hamilton's precept general form was used [41]:

$$\delta\int_{t_1}^{t_2}(P_E - K_E)dt = 0 \tag{6}$$

Substituting the potential energy (4) and kinetic energy (5) into Hamilton's precept equation (6) and then applying integration by parts gives the vibration equation of a bidirectional graded cracked Rayleigh beam as

$$EI_{eq}\left[f_1(x)\frac{\partial^4 w_1}{\partial x^4} + 2\frac{\partial f_1(x)}{\partial x}\frac{\partial^3 w_1}{\partial x^3} + \frac{\partial^2 f_1(x)}{\partial x^2}\frac{\partial^2 w_1}{\partial x^2}\right] + f_2(x)\rho A_{eq}\frac{\partial^2 w_1}{\partial t^2} - f_2(x)\rho I_{eq}\frac{\partial^4 w_1}{\partial x^2 \partial t^2} - \frac{\partial f_2(x)}{\partial x}\rho I_{eq}\frac{\partial^3 w_1}{\partial x \partial t^2} = 0 \quad at \quad 0 \le x \le x_c \tag{7a}$$

$$EI_{eq}\left[f_1(x)\frac{\partial^4 w_2}{\partial x^4} + 2\frac{\partial f_1(x)}{\partial x}\frac{\partial^3 w_2}{\partial x^3} + \frac{\partial^2 f_1(x)}{\partial x^2}\frac{\partial^2 w_2}{\partial x^2}\right] + f_2(x)\rho A_{eq}\frac{\partial^2 w_2}{\partial t^2} - f_2(x)\rho I_{eq}\frac{\partial^4 w_2}{\partial x^2 \partial t^2} - \frac{\partial f_2(x)}{\partial x}\rho I_{eq}\frac{\partial^3 w_2}{\partial x \partial t^2} = 0 \ at \ ; \ x_c \le x \le L \tag{7b}$$

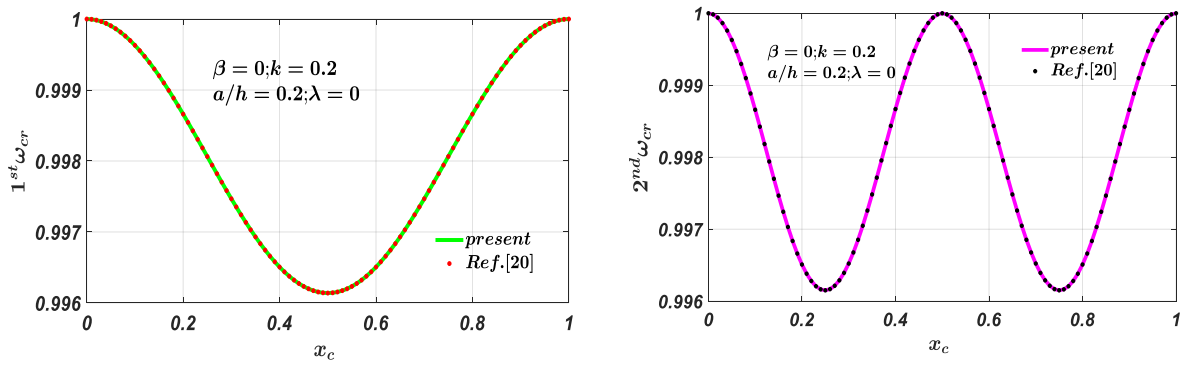


**Fig. 4.** First and second cracked frequency ratio for FGM Euler beam.

in which

$$\left.\begin{aligned} EI_{eq} &= b\int_{-h/2}^{h/2}\left((E_c-E_m)\left(\frac{z}{h}+\frac{1}{2}\right)^{p}+E_m\right)z^2dz = E_mI\gamma \\ \rho A_{eq} &= b\int_{-h/2}^{h/2}\left((\rho_c-\rho_m)\left(\frac{z}{h}+\frac{1}{2}\right)^{p}+\rho_m\right)dz = \rho_m A\alpha_1 \\ \rho I_{eq} &= b\int_{-h/2}^{h/2}z^2\left((\rho_c-\rho_m)\left(\frac{z}{h}+\frac{1}{2}\right)^{p}+\rho_m\right)dz = \rho_m I\alpha_2 \end{aligned}\right\} \tag{8}$$

For the 2D FG beam simply supported at both ends:

$$\left.\begin{aligned} w(0,t) &= \frac{\partial^2 w(0,t)}{\partial x^2} = 0, at\ x = 0 \\ w(L,t) &= \frac{\partial^2 w(L,t)}{\partial x^2} = 0, at\ x = L \end{aligned}\right\} \tag{9}$$

The following dimensionless quantities are introduced:

$$\xi = \frac{x}{L}, \xi_c = \frac{x_c}{L}, \eta_1 = \frac{w_1}{L}, \eta_2 = \frac{w_2}{L};\ \tau = t \bullet \sqrt{L^4 \bullet \frac{\rho_m A}{E_m I}}, \lambda = \frac{I}{AL^2} \tag{10}$$

Substituting equations (2), (8) and (18) into equation (7), the final dimensionless equations of a cracked bidirectional graded Rayleigh beam model are given as

$$\begin{aligned} &\alpha_1\ e^{\beta\xi}\ \frac{\partial^2\eta_1}{\partial\tau^2} - \lambda\ \alpha_2\ e^{\beta\xi}\ \frac{\partial^4\eta_1}{\partial\xi^2\partial\tau^2} - \lambda\ \alpha_2\beta e^{\beta\xi}\frac{\partial^3\eta_1}{\partial\xi\partial\tau^2} \\ &+ e^{\beta\xi}\ \gamma\left(\frac{\partial^4\eta_1}{\partial\xi^4} + 2\beta\ \frac{\partial^3\eta_1}{\partial\xi^3} + \beta^2\ \frac{\partial^2\eta_1}{\partial\xi^2}\right) = 0, at \quad 0 \le \xi \le \xi_c \end{aligned} \tag{11a}$$

$$\begin{aligned} &\alpha_1\ e^{\beta\xi}\ \frac{\partial^2\eta_2}{\partial\tau^2} - \lambda\ \alpha_2\ e^{\beta\xi}\ \frac{\partial^4\eta_2}{\partial\xi^2\partial\tau^2} - \lambda\ \alpha_2\beta e^{\beta\xi}\frac{\partial^3\eta_2}{\partial\xi\partial\tau^2} \\ &+ e^{\beta\xi}\ \gamma\left(\frac{\partial^4\eta_2}{\partial\xi^4} + 2\beta\ \frac{\partial^3\eta_2}{\partial\xi^3} + \beta^2\ \frac{\partial^2\eta_2}{\partial\xi^2}\right) = 0, at \quad \xi_c \le \xi \le 1 \end{aligned} \tag{11b}$$

Substituting equation (10) into equation (9), the dimensionless form of boundary conditions can be expressed as:

$$\left.\begin{aligned} \xi = 0, \eta(0,T) &= \frac{\partial^2\eta(0,T)}{\partial\xi^2} = 0 \\ \xi = 1, \eta(1,T) &= \frac{\partial^2\eta(1,T)}{\partial\xi^2} = 0 \end{aligned}\right\} \tag{12}$$

## 3. Solution method

The Galerkin method is employed to separate the time and space dimensions of the system, as well as to transform the system's partial differential equations into ordinary differential equations. Within this method, the system's lateral displacements are approximated by the following expressions [42].

$$\eta(\xi,T) = \sum_{r=1}^{n}\varphi_r(\xi)q_r(T) \tag{13}$$

The cracked simply supported FG beam mode shape is written as [36, 43].

$$\varphi_{r1}(\xi) = \varphi(\xi) + A_o + A_1\xi + A_2\xi^2 + A_3\xi^3 \text{ for } 0 \le \xi \le \xi_c \tag{14a}$$

$$\varphi_{r2}(\xi) = \varphi(\xi) + B_o + B_1\xi + B_2\xi^2 + B_3\xi^3 \text{ for } \xi_c \le \xi \le 1 \tag{14b}$$

The cracked FG beam continuity and compatibility conditions are written as [44].

$$\left.\begin{aligned} \varphi_{r1}(\xi_c) &= \varphi_{r2}(\xi_c) \\ \varphi''_{r1}(\xi_c) &= \varphi''_{r2}(\xi_c) \\ \varphi'''_{r1}(\xi_c) &= \varphi'''_{r2}(\xi_c) \\ \varphi'_{r2}(\xi_c) - \varphi'_{r1}(\xi_c) &= K\varphi''_{r2}(\xi_c) \end{aligned}\right\} \tag{15}$$

where $c$ in equation (15) is written as [31]

$$K = 6\pi(1-\nu^2)h\gamma f(a/h) \tag{16}$$

In terms of crack depth ratio (a/h), $f(a/h)$ can be expressed as [45]

$$\begin{aligned} f(a/h) &= 0.6272(a/h)^2 - 1.04533(a/h)^3 + 4.5948(a/h)^4 \\ &-9.9736(a/h)^5 + 20.2948(a/h)^6 - 33.0351(a/h)^7 \\ &+47.1063(a/h)^8 - 40.7556(a/h)^9 + 19.6(a/h)^{10} \end{aligned} \tag{17}$$

Inserting the derivatives of equation (14) into equations (12) and (15), and after some mathematical manipulation, the final mode shape is written as:

$$\varphi_{r1}(\xi) = sin(n\pi\xi) - \left(\frac{\xi_c - 1}{\xi_c}\right)\left[K\xi_c(n\pi)^2 sin(n\pi\xi_c)\right]\xi\ at\ \ (0 \le \xi \le \xi_c) \tag{18a}$$

$$\varphi_{r2}(\xi) = sin(n\pi\xi) + (1-\xi)\left[K\xi_c(n\pi)^2 sin(n\pi\xi_c)\right]\ at\ (\xi_c \le \xi \le 1) \tag{18b}$$

By multiplying both sides of the dynamic equations of the system by the shape functions of the vibrational mode, integrating over the length of the beam, and using the orthogonal property of the vibrational modes, the dynamical equations of the system in matrix form are expressed as follows:

$$[M]\ddot{q} + [K]q = 0, q = (q)^T \tag{19}$$

where in

$$M(r,s)=\left\{\alpha_1\int_0^{\xi_c}\left[e^{\beta\xi}\varphi_{r1}(\xi)\varphi_{s1}(\xi)\right]d\xi-\lambda\alpha_2\int_0^{\xi_c}[\varphi_{r1}{}''(\xi)\varphi_{s1}(\xi)]d\xi\int_0^{\xi_c}\left[e^{\beta\xi}\varphi_{r1}(\xi)\varphi_{s1}(\xi)\right]d\xi-\lambda\beta\alpha_2\int_0^{\xi_c}[\varphi_{r1}{}'(\xi)\varphi_{s1}(\xi)]d\xi\int_0^{\xi_c}\left[e^{\beta\xi}\varphi_{r1}(\xi)\varphi_{s1}(\xi)\right]d\xi\right\}$$
$$+\left\{\alpha_1\int_{\xi_c}^{1}\left[e^{\beta\xi}\varphi_{r2}(\xi)\varphi_{s2}(\xi)\right]d\xi-\lambda\alpha_2\int_{\xi_c}^{1}[\varphi_{r2}{}''(\xi)\varphi_{s2}(\xi)]d\xi\int_{\xi_c}^{1}\left[e^{\beta\xi}\varphi_{r2}(\xi)\varphi_{s2}(\xi)\right]d\xi-\lambda\beta\alpha_2\int_{\xi_c}^{1}[\varphi_{r2}{}'(\xi)\varphi_{s2}(\xi)]d\xi\int_{\xi_c}^{1}\left[e^{\beta\xi}\varphi_{r2}(\xi)\varphi_{s2}(\xi)\right]d\xi\right\} \tag{20a}$$

$$K(r,s)=\left\{\gamma\int_0^{\xi_c}e^{\beta\xi}\varphi_{r1}{}^{iv}(\xi)\varphi_{s1}(\xi)d\xi+2\beta\gamma\int_0^{\xi_c}e^{\beta\xi}\varphi_{r1}{}'''(\xi)\varphi_{s1}(\xi)d\xi+\gamma\beta^2\int_0^{\xi_c}e^{\beta\xi}\varphi_{r1}{}''(\xi)\varphi_{s1}(\xi)d\xi\right\}$$
$$+\left\{\gamma\int_{\xi_c}^{1}e^{\beta\xi}\varphi_{r2}{}^{iv}(\xi)\varphi_{s2}(\xi)d\xi+2\beta\gamma\int_{\xi_c}^{1}e^{\beta\xi}\varphi_{r2}{}'''(\xi)\varphi_{s2}(\xi)d\xi+\gamma\beta^2\int_{\xi_c}^{1}e^{\beta\xi}\varphi_{r2}{}''(\xi)\varphi_{s2}(\xi)d\xi\right\} \tag{20b}$$

To determine the natural frequencies, the system is transformed into the state space, and a state vector is defined as follows $X(T)=\begin{bmatrix}q^T(t) & q^{\bullet T}(t)\end{bmatrix}$. The equation in the state space is obtained as follows [32]:

$$\dot{X}(T)=BX(T) \tag{21}$$

where;

$$B=\begin{bmatrix}0 & \vdots & I\\ \cdots & \vdots & \cdots\\ -M^{-1}*K & \vdots & 0\end{bmatrix} \tag{22}$$

B is a matrix with constant coefficients. Then consider the solution of the vibrating system as $X(T)=e^{\lambda t}x$ and put it in the previous equation and divide by $e^{\lambda t}$, we get

$$Ax=\lambda x \tag{23}$$

The algebraic eigenvalue problem, equation (23), is a basic theory in vibrational problems, and the eigenvalues represent the frequencies of the system.

## 4. Validation study

This study presents three explicit examples to validate the proposed solution for predicting the free vibration analysis of cracked bidirectionally functionally graded material (BDFGM) Rayleigh beams. First, the intact functionally graded material (FGM) Euler beam results are validated. The beam in this validity is composed of AL (metal) and $Al_2O_3$ (ceramic), and the first four natural frequencies are calculated using the formula in equation (24). The present results when using Galerkin's method are compared to those in Ref. [46], as shown in Table 1. A reasonable agreement was found. The non-dimensional frequencies, expressed by the following relation, are useful for reporting numerical results and comparing them to the findings in the technical literature.

$$\varpi=\omega L^2\sqrt{\frac{\rho_m A}{E_m I}} \tag{24}$$

To further validate the proposed Galerkin technique, the third example is done with a cracked FGM beam fabricated of aluminum ($AL$) and alumina ($Al_2O_3$), as also presented in Ref. [31]. The frequency ratio for cracked to un-cracked FG Euler beam was compared to the results in Ref. [31] at $a/h=0.2$ as tabulated in Fig. 2 for the first and second modes. From this figure, it is shown that a good agreement was found. From the verified above, it is observed that Galerkin's method can be effectively used to solve the complicated vibration equation (23).

In a similar way, the first four vibration frequencies of the uncracked FGM Euler-Bernoulli beam have been presented in Table 2 with $E_\rho=0.5$ and 2.0 and $k=0,0.1,2.0$ and constant mass density and compared with [47,48]. It is clear that the computations present good agreement. This can be observed in the precision of the results, as well as in the consistency of the numbers. This agreement is further emphasized when comparing the computations with each other.

**Table 1**
First fourth dimensionless frequencies of FGM beams.

| *Mode No.* | *Source* | Frequency dimensionless parameter ($\varpi$) | | |
|---|---|---|---|---|
| | | *Thickness gradient* ($k$) | | |
| | | 0.1 | 1 | 5 |
| $1^{st}$ | *Present* | 17.604 | 13.586 | 11.423 |
| | Ref. [46] | 17.594 | 13.384 | 11.367 |
| $2^{nd}$ | *Present* | 70.417 | 53.546 | 45.510 |
| | Ref. [46] | 70.367 | 53.547 | 45.481 |
| $3^{rd}$ | *Present* | 158.440 | 120.602 | 120.412 |
| | Ref. [46] | 158.376 | 120.58 | 120.40 |
| $4^{th}$ | *Present* | 281.471 | 214.720 | 182.323 |
| | Ref. [46] | 281.300 | 214.690 | 182.290 |

### 4.1. Numerical results

Natural frequencies have been computed using MATLAB's version (R2015a) in accordance with the Galerkin technique described above. A study is conducted on the frequency of graded beams with and without cracks. In the following numerical examples, the dimensions used in the calculation for the FG beam are given as the beam width $b=0.1m$, the beam height $h=0.02m$, and the beam length $L=1m$ [24]. FGM beams comprised of Stainless steel (SUS304) metal ($k=\infty$) and Alumina ($Al2O3$) ceramics ($k=0$) were used here, and the material beam properties are as:

$$E_m=210\ GPa\ ;\ E_c=390\ GPa;\ \ \rho_m=8166 kg/m^3\ ;\ \ and\ \ \ \rho_c=3960\ kg/m^3.$$

### 4.2. Effect of thickness and axial gradient

This subsection illustrates the power-law and axial indexes impact on the three first frequencies of the uncracked Rayleigh FGM beam (i.e., $x_c=0$ and $d_c=0$) as shown in Table 3. This table indicates that the dimensionless natural frequencies affect by the property gradient index ($k$) of the FGM beam with simply-simply end conditions for different values of axial gradient index ($\beta$). The results show that the natural frequencies of the FGM beam decreased as the composition index increased. This behavior is because a decrease in the ceramic material relative to the metal material inside the beam makes the beam more

**Table 2**
Comparison of the first-fourth nondimensional frequencies of FGM beams.

| Modules ratio $E_\rho$ | Gradient index $k$ | Method | Non-dimensional Frequency ($\sqrt{\varpi}$) | | | |
|---|---|---|---|---|---|---|
| | | | $1^{st}$ | $2^{nd}$ | $3^{rd}$ | $4^{th}$ |
| $E_\rho = 0.5$ | $k = 0$ | Present | 2.64175 | 5.28351 | 7.92526 | 10.567 |
| | | DQM [47] | 2.6418 | 5.2836 | 7.9258 | 10.5692 |
| | | Analytical [48] | 2.6416 | 5.283 | 7.9237 | – |
| | $k = 0.1$ | Present | 2.71527 | 5.43054 | 8.14581 | 10.8611 |
| | | DQM [47] | 2.7153 | 5.4306 | 8.1464 | 10.8633 |
| | | Analytical [48] | 2.7117 | 5.4232 | 8.1339 | – |
| | $k = 2$ | Present | 2.97113 | 5.94227 | 8.9134 | 11.8845 |
| | | DQM [47] | 2.9711 | 5.9424 | 8.914 | 11.887 |
| | | Analytical [48] | 2.9475 | 5.8947 | 8.8411 | – |
| $E_\rho = 2$ | $k = 0$ | Present | 3.736 | 7.47201 | 11.208 | 14.944 |
| | | DQM [47] | 3.736 | 7.4721 | 11.2088 | 14.9471 |
| | | Analytical [48] | 3.7359 | 7.4713 | 11.2059 | – |
| | $k = 0.1$ | Present | 3.68059 | 7.36118 | 11.0418 | 14.7224 |
| | | DQM [47] | 3.6806 | 7.3613 | 11.0425 | 14.7254 |
| | | Analytical [48] | 3.6793 | 7.3582 | 11.0362 | – |
| | $k = 2$ | Present | 3.41729 | 6.83458 | 10.2519 | 13.6692 |
| | | DQM [47] | 3.4173 | 6.8347 | 10.2526 | 13.672 |
| | | Analytical [48] | 3.3784 | 6.7563 | 10.1333 | – |

**Table 3**
First three dimensionless natural frequencies with different $k$ *and* $\beta$.

| *Axial index* $\beta$ | *Frequency No.* | *Gradient index k* | | | | | |
|---|---|---|---|---|---|---|---|
| | | 0 | 0.5 | 1 | 3 | 5 | 10 |
| 0 | 1 | 18.008 | 14.232 | 12.961 | 11.493 | 10.996 | 10.436 |
| | 2 | 63.933 | 50.392 | 46.016 | 41.027 | 39.284 | 37.2466 |
| | 3 | 123.632 | 97.195 | 88.985 | 79.765 | 76.434 | 72.399 |
| 0.5 | 1 | 17.960 | 14.194 | 12.927 | 11.923 | 10.967 | 10.408 |
| | 2 | 63.816 | 50.297 | 45.932 | 42.531 | 39.217 | 37.1823 |
| | 3 | 123.104 | 96.773 | 88.605 | 82.353 | 76.121 | 72.1008 |
| 1 | 1 | 17.818 | 14.081 | 12.824 | 11.372 | 10.881 | 10.326 |
| | 2 | 63.459 | 50.008 | 45.675 | 40.740 | 39.011 | 36.985 |
| | 3 | 121.511 | 95.501 | 87.458 | 78.441 | 75.172 | 71.197 |

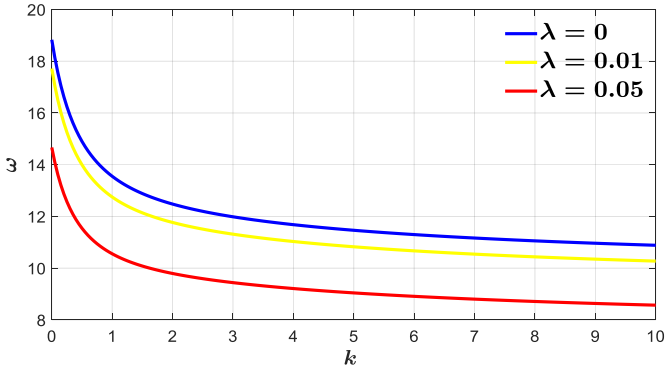


**Fig. 5.** First mode variation against gradient index with different Rayleigh parameter ($\lambda$).

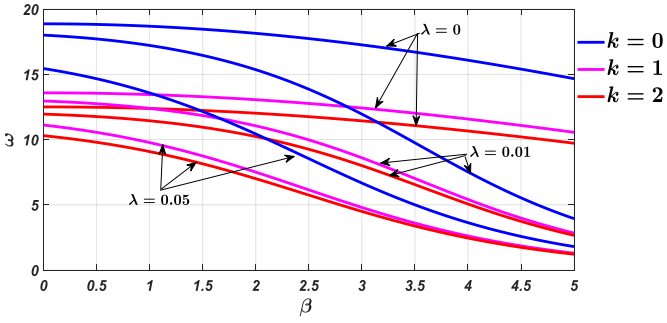


**Fig. 6.** Variation of first dimensionless frequency versus axial index with different values of power index and Rayleigh factor.

flexible, decreasing the vibration frequencies. At the same time, in this table, it is also shown that when the longitudinal index increases, the frequencies are decreased.

Furthermore, the impact of the volume fraction exponent on the first frequency of uncracked FGM beam with distinct Rayleigh parameters ($\lambda$) is demonstrated in Fig. 5. As evidenced by the figure, the dimensionless frequencies are influenced by the Rayleigh parameter as well as the FGM beam's property gradient index ($k$) with simply supported end conditions.

Fig. 6 clearly demonstrates the influence of the Rayleigh parameter on the non-dimensional frequencies of the intact FG beam for three different values of thickness index ($k = 0, 1, 2$). The results show that as the Rayleigh factor increases, the frequency decreases in a varying manner. When the Rayleigh parameter is set to $a = 0.05$, the frequencies change more rapidly than when the Rayleigh factor is set to a lower value. This suggests that the Rayleigh parameter significantly impacts the non-dimensional frequencies of an intact FG beam.

### 4.3. *Effect of crack location* ($xc$ /$L$)

This subsection describes the impact of the position of cracks on the vibration frequency of the bidirectionally graded Rayleigh beam model with simply-supported end conditions with different crack depth ratios and composition indices. The presence of a crack at a specific location along the beam leads to an increase or decrease in the natural frequencies of the beam depending on the proximity or distance of the

**Table 4**
Effect of crack location and depth ratio on the first and second natural frequencies at ($\lambda = 0.05, \beta = 0.5$).

| *Crack position ratio* ($\xi_c$) | *Crack depth ratio* ($a/h$) | *Composition index* ($k$) | | | | | | | |
|---|---|---|---|---|---|---|---|---|---|
| | | 0 | | 0.5 | | 1 | | 2 | |
| | | $\lambda_1$ | $\lambda_2$ | $\lambda_1$ | $\lambda_2$ | $\lambda_1$ | $\lambda_2$ | $\lambda_1$ | $\lambda_2$ |
| 0.1 | 0.1 | 15.387 | 43.490 | 12.121 | 34.106 | 11.076 | 31.313 | 10.265 | 29.218 |
| | 0.3 | 15.308 | 42.655 | 12.070 | 33.588 | 11.033 | 30.883 | 10.228 | 28.850 |
| | 0.5 | 15.073 | 30.962 | 11.919 | 28.831 | 10.906 | 28.755 | 10.118 | 27.753 |
| 0.3 | 0.1 | 15.32 | 43.267 | 12.077 | 33.964 | 11.039 | 31.193 | 10.233 | 29.114 |
| | 0.3 | 14.7027 | 35.195 | 11.672 | 31.859 | 10.697 | 29.570 | 9.937 | 27.546 |
| | 0.5 | 8.024 | 11.074 | 7.815 | 10.374 | 7.818 | 10.133 | 7.811 | 9.708 |
| 0.5 | 0.1 | 15.272 | 43.543 | 12.045 | 34.140 | 11.012 | 31.342 | 10.210 | 29.243 |
| | 0.3 | 14.318 | 24.713 | 11.413 | 23.438 | 10.477 | 23.322 | 9.746 | 23.329 |
| | 0.5 | 5.765 | 8.703 | 5.673 | 8.047 | 5.725 | 7.880 | 5.792 | 7.725 |

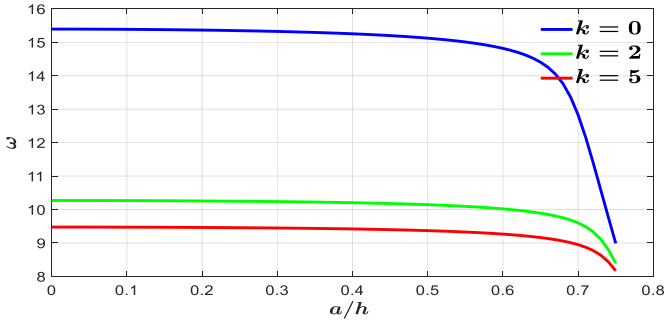


**Fig. 7.** First mode variation against crack length ratio with different gradient index.

crack location to the beam end supports, as shown in Table 4. Additionally, from this table, it can be seen that when the gradient index increases, the natural frequency decreases due to the increase in metal components relative to ceramic components, which leads to a decrease in beam stiffness. It is also noted from this table that the first two frequencies decrease when the crack depth ratio increases. This is because the crack's presence reduces the beam's stiffness and therefore reduces vibrations.

Moreover, the influence of the crack depth ($alh$) ratio on the first nondimensional frequency with a different gradient index ($k$) is depicted in Fig. 7. As expected, it is shown that when the ratio of crack depth increases, the fundamental frequency decreases. At the same time, it is observed that when the gradient index increases, the first frequency decreases.

Furthermore, the first natural frequencies against the crack position along the beam length with various crack depth ratios, thickness gradients, and axial gradients are illustrated in Figs 8a, 8b and 8c. These figures show that natural frequencies decrease as the crack depth ratio increases. When the crack depth ratio increases, the beam stiffness lowers, decreasing the beam's natural frequency.

Also, as per Fig. 8a, if the crack location shifts from the support to the middle of the beam, the natural frequency consistently decreases for all crack depths. Similarly, changing the crack location from the middle to the opposite support results in an increase in the frequency value.

### 4.4. *Effect of modulus and density ratio*

The effect of the modulus of elasticity $E_\rho$ and density $R_\rho$ ratio of ceramic to the metal on the natural frequencies of simply supported bidirectional graded uncracked and cracked beam models for different power-index and axial gradient indices are demonstrated in this subsection.

Fig. 9 demonstrates the fundamental dimensionless frequencies of cracked Rayleigh BDFGM beams against the effective modulus ratio $E_\rho$ with different rotary inertia factors $\lambda$. The results show that the frequencies increase with an increasing effective modulus ratio. This is because increased effective modulus ratio results in increased stiffness of

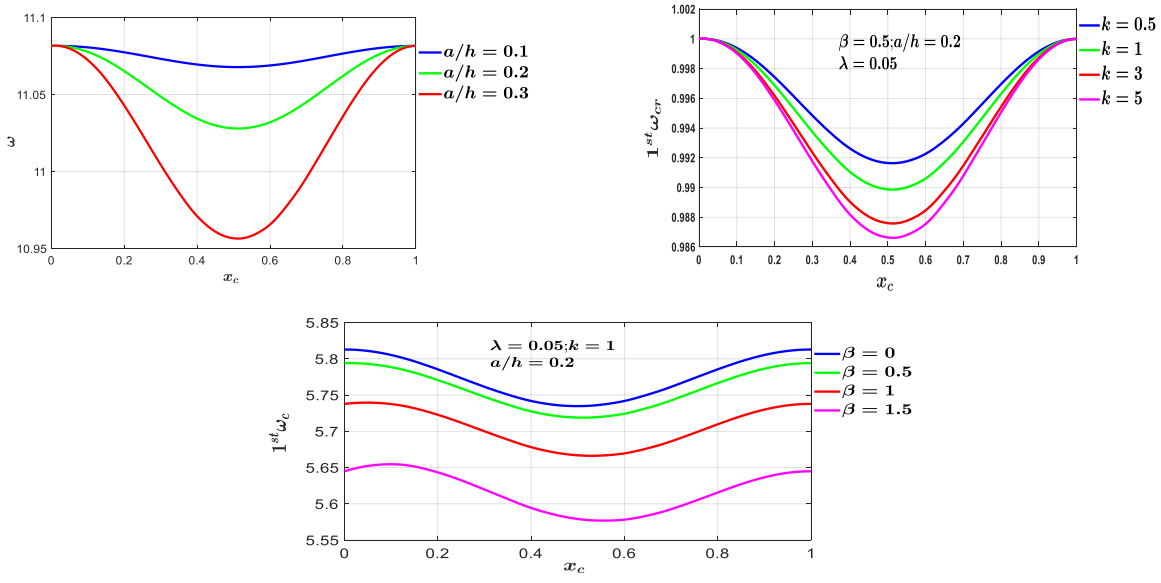


**Fig. 8.** The impact of the crack position ratio toward first mode frequency for different ($a/h$) ratios, thickness index ($k$), and axial index, respectively.

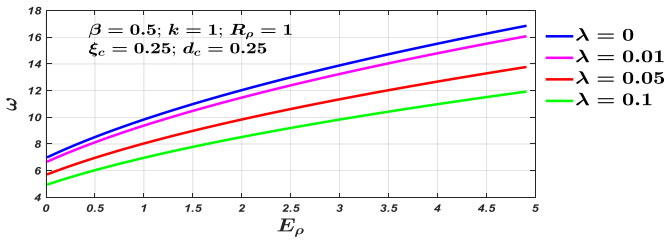


**Fig. 9.** Variation of first mode frequency versus modulus ratio with different Rayleigh factor.

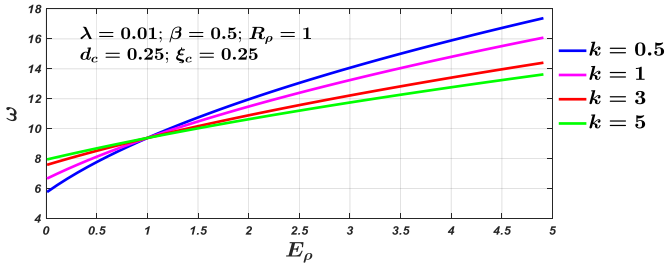


**Fig. 10.** First vibration frequency variation versus modulus ratio with different power exponent.

the beam and hence an increase in its natural frequency. At the same time, this figure demonstrates that this frequency decrease can be attributed to the mass-addition effect of the rotary inertia factor. As rotary inertia increases, the beam's mass increases, decreasing its natural frequency. Therefore, it can be concluded that rotary inertia directly affects Rayleigh BDFGM beam natural frequency.

Fig. 10 shows the effect of the modulus ratio $E_\rho$ on the first mode frequency of cracked Rayleigh BDFGM beams in relation to different power law exponents. It is observed that when the modulus ratio is increased, the fundamental frequency increases significantly at the lower power exponent values. However, there is little to no change in the fundamental frequency when higher power exponent values are considered, regardless of the modulus ratio. This indicates that the modulus ratio has a more significant effect on the frequency of the beam with smaller power law exponents. As shown in Fig. 10, it is evident that the natural frequencies of the FG beams increase with the increase of parameter $k$ when $E_\rho$ is less than 1. In contrast, when $E_\rho$ is greater than 1, the natural frequencies of the FG beams decrease when parameter $k$ increases. This trend can be seen throughout the range of parameter $k$. Thus, it is clear that the natural frequencies of the FG beams depend on the value of the parameter $k$ and the $E_\rho$.

Table 5 presents non-dimensional frequencies under the effect of modulus of elasticity $E_\rho$ ratio rises and crack position ratio $\xi_c$ for the first three modes of vibration of cracked BDFGM beam. In this table, the results are presented for $k = 1;\ \lambda = 0.01;\ \beta = 0.5;$ and $d_c = 0.2$. This table clearly demonstrates that when the crack location in the beam increases, there is a proportional decrease in the corresponding non-dimensional frequencies. This is because the presence of the crack reduces the beam stiffness, thereby decreasing the frequencies. The evidence presented in this table indicates that the location of a crack in a beam significantly influences the beam's stiffness and non-dimensional frequencies.

Fig. 11 shows the effect of density ratios $R_\rho$ on the frequency of a cracked Rayleigh BDFGM beam with different power law exponents. It is evident from this figure that the frequency decreases significantly with an increasing density ratio. This is due to the added mass from the increasing density ratio, which results in a decrease of the fundamental frequency. It can be seen that the largest decrease in frequency occurs with the largest density ratio. The results demonstrate that the density

**Table 5**
Effect of crack position ratio on the first three-order natural frequency with different modulus ratio at $(\lambda = 0.05, \beta = 0.5, k = 1)$.

| *Effective modulus ratio* $E_R$ | *Frequency No.* | Crack position ratio $\xi_c$ | | |
|---|---|---|---|---|
| | | $\xi_c$=0 | $\xi_c$=0.15 | $\xi_c$=0.25 |
| $E_R = 0.2$ | 1 | 7.2741 | 7.2719 | 7.2684 |
| | 2 | 25.8456 | 25.8251 | 25.8086 |
| | 3 | 49.8572 | 49.7598 | 49.7038 |
| $E_R = 0.5$ | 1 | 8.1327 | 8.1297 | 8.1247 |
| | 2 | 28.8963 | 28.8676 | 28.8445 |
| | 3 | 55.7421 | 55.6050 | 55.5665 |
| $E_R = 1$ | 1 | 9.3909 | 9.3861 | 9.3785 |
| | 2 | 33.3666 | 33.3223 | 33.2864 |
| | 3 | 64.3654 | 64.2519 | 64.2464 |
| $E_R = 2$ | 1 | 11.5014 | 11.4927 | 11.4788 |
| | 2 | 40.8655 | 40.7835 | 40.7171 |
| | 3 | 78.8312 | 78.6301 | 78.6032 |
| $E_R = 5$ | 1 | 16.2655 | 16.2409 | 16.2015 |
| | 2 | 57.7926 | 57.5559 | 57.3625 |
| | 3 | 111.4842 | 110.2775 | 110.1613 |

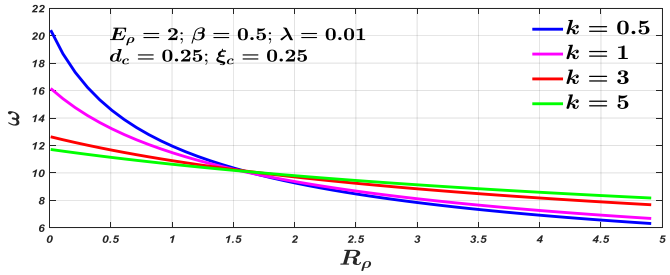


**Fig. 11.** First vibration frequency variation versus density ratio with different power exponent.

ratio has a significant impact on the frequency of the beam. Also, Figure (11) shows that as the gradient index increases, the frequency for $R_\rho < 1.56$ decreases and this behavior is reversed in $R_\rho > 1.56$.

## 5. Conclusions

The vibration characteristics of a cracked Rayleigh beam comprised of bidirectionally functionally graded material (BDFGM) were analyzed in this study using Hamilton's principle and the Galerkin method. The study investigated the impact of distinct parameters, such as the gradient index, crack depth ratio, crack position, and Rayleigh parameter $(\lambda)$, on the natural frequencies of the cracked beam. The study results led to the following conclusions:

1 The natural frequencies of the intact and cracked bidirectionally graded beams decreased as the gradient index increased.
2 The natural frequencies of the BDFGM beam decreased as the crack depth ratio and crack position increased.
3 The presence of a crack in the FG beam distorted the symmetry of the vibration mode shape and reduced the natural frequencies, with greater reductions occurring at mid-distance crack locations.
4 The vibration frequencies of the FG beam decreased with increasing values of the Rayleigh parameter $(\lambda)$ and were further reduced in the presence of a crack.

The suggestion for the future direction is a temperature gradient effect which can be added to the current study as well as an external excitation force.

## Credit author statement

**Talib EH. Elaikh**: Conceptualization, Methodology / Study design,

Formal analysis, Resources, Writing – original draft, Supervision, **Nada M. Abd**: Conceptualization, Methodology / Study design, Validation, Investigation, Resources, Writing – original draft, **Ali Hasan Al**: Conceptualization, Methodology / Study design, Formal analysis, Software, Writing – review & editing, Project administration.

## Declaration of competing interest

The authors declare that they have no known competing financial interests or personal relationships that could have appeared to influence the work reported in this paper.

## Data availability

No data was used for the research described in the article.

## References


[1] A. Karamanlı, Free vibration analysis of two directional functionally graded beams using a third order shear deformation theory, Compos. Struct. 189 (August 2017) (2018) 127–136, https://doi.org/10.1016/j.compstruct.2018.01.060.

[2] S.M. Ihmood, T.E. Elaikh, M. Al-Umar, Free vibration of new type functionally graded materials pipe conveying fluid using differential quadrature method, AIP Conf. Proc. 2386 (January) (2022), https://doi.org/10.1063/5.0066803.

[3] S.R. Li, Z.Q. Wan, J.H. Zhang, Free vibration of functionally graded beams based on both classical and first-order shear deformation beam theories, Appl. Math. Mech. (English Ed. 35 (5) (2014) 591–606, https://doi.org/10.1007/s10483-014-1815-6.

[4] T.E.H. Elaikh, N.M. Abed, A. Ebrahimi-Mamaghani, Free vibration and flutter stability of interconnected double graded micro pipes system conveying fluid, IOP Conf. Ser. Mater. Sci. Eng. 928 (2) (2020), https://doi.org/10.1088/1757-899X/928/2/022128.

[5] M. Aydogdu, Semi-inverse method for vibration and buckling of axially functionally graded beams, J. Reinforc. Plast. Compos. 27 (7) (2008) 683–691, https://doi.org/10.1177/0731684407081369.

[6] N.M.A. Talib, E.H. Elaikh, Stability of FG material micro-pipe conveying fluid 10 (4) (2019) 211–222.

[7] M. Aydogdu, V. Taskin, Free vibration analysis of functionally graded beams with simply supported edges, Mater. Des. 28 (5) (2007) 1651–1656, https://doi.org/10.1016/j.matdes.2006.02.007.

[8] S.C. Mohanty, R.R. Dash, T. Rout, Static and dynamic stability analysis of a functionally graded timoshenko beam, Int. J. Struct. Stabil. Dynam. 12 (4) (2012) 1–33, https://doi.org/10.1142/S0219455412500253.

[9] N. Wattanasakulpong, V. Ungbhakorn, Free vibration analysis of functionally graded beams with general elastically end constraints by DTM, World J. Mech. 2 (6) (2012) 297–310, https://doi.org/10.4236/wjm.2012.26036.

[10] H.T. Thai, T.P. Vo, Bending and free vibration of functionally graded beams using various higher-order shear deformation beam theories, Int. J. Mech. Sci. 62 (1) (2012) 57–66, https://doi.org/10.1016/j.ijmecsci.2012.05.014.

[11] Ö. Civalek, Ş.D. Akbaş, B. Akgöz, S. Dastjerdi, Forced vibration analysis of composite beams reinforced by carbon nanotubes, Nanomaterials 11 (3) (2021) 1–17, https://doi.org/10.3390/nano11030571.

[12] Y.S. Al Rjoub, A.G. Hamad, Free vibration of functionally Euler-Bernoulli and Timoshenko graded porous beams using the transfer matrix method, KSCE J. Civ. Eng. 21 (3) (2017) 792–806, https://doi.org/10.1007/s12205-016-0149-6.

[13] H. Ziou, H. Guenfoud, M. Guenfoud, Numerical modelling of a Timoshenko FGM beam using the finite element method, Int. J. Struct. Eng. 7 (3) (2016) 239–261, https://doi.org/10.1504/IJSTRUCTE.2016.077719.

[14] J.W. Lee, J.Y. Lee, Free vibration analysis of functionally graded Bernoulli-Euler beams using an exact transfer matrix expression, Int. J. Mech. Sci. 122 (2017) 1–17, https://doi.org/10.1016/j.ijmecsci.2017.01.011.

[15] B. Akgöz, Ö. Civalek, A novel microstructure-dependent shear deformable beam model, Int. J. Mech. Sci. 99 (2015) 10–20, https://doi.org/10.1016/j.ijmecsci.2015.05.003.

[16] J.R. Banerjee, A. Ananthapuvirajah, Free vibration of functionally graded beams and frameworks using the dynamic stiffness method, J. Sound Vib. 422 (2018) 34–47, https://doi.org/10.1016/j.jsv.2018.02.010.

[17] D. Bonthu, V. Mahesh, S. Powar, M. Doddamani, 3D printed functionally graded foams response under transverse load, Results Mater 19 (June) (2023), 100410, https://doi.org/10.1016/j.rinma.2023.100410.

[18] F. Rahmani, R. Kamgar, R. Rahgozar, Finite element analysis of functionally graded beams using different beam theories, Civ. Eng. J. 6 (11) (2020) 2086–2102, https://doi.org/10.28991/cej-2020-03091604.

[19] M. Şimşek, Buckling of Timoshenko beams composed of two-dimensional functionally graded material (2D-FGM) having different boundary conditions, Compos. Struct. 149 (2016) 304–314, https://doi.org/10.1016/j.compstruct.2016.04.034.

[20] A.E. Alshorbagy, M.A. Eltaher, F.F. Mahmoud, Free vibration characteristics of a functionally graded beam by finite element method, Appl. Math. Model. 35 (1) (2011) 412–425, https://doi.org/10.1016/j.apm.2010.07.006.

[21] Y. Lu, X. Chen, Nonlinear parametric dynamics of bidirectional functionally graded beams, Shock Vib. 2020 (2020), https://doi.org/10.1155/2020/8840833.

[22] S. Rajasekaran, H.B. Khaniki, Free vibration analysis of bi-directional functionally graded single/multi-cracked beams, Int. J. Mech. Sci. 144 (2018) 341–356, https://doi.org/10.1016/j.ijmecsci.2018.06.004.

[23] X. Zhao, Free vibration analysis of cracked Euler-Bernoulli beam by laplace transformation considering stiffness reduction, Rom. J. Acoust. Vib. 16 (2) (2019) 166–173.

[24] G. Tan, J. Shan, C. Wu, W. Wang, Direct and inverse problems on free vibration of cracked multiple I-section beam with different boundary conditions, Adv. Mech. Eng. 9 (11) (2017) 1–17, https://doi.org/10.1177/1687814017737261.

[25] A.S.J. Swamidas, X. Yang, R. Seshadri, Identification of cracking in beam structures using timoshenko and euler formulations, J. Eng. Mech. 130 (November) (2004) 1297–1308, https://doi.org/10.1061/(ASCE)0733-9399(2004)130.

[26] Ş.D. Akbaş, Free vibration of edge cracked functionally graded microscale beams based on the modified couple stress theory, Int. J. Struct. Stabil. Dynam. 16 (10) (2016) 1–23, https://doi.org/10.1142/S021945541750033X.

[27] H.P. Lin, Direct and inverse methods on free vibration analysis of simply supported beams with a crack, Eng. Struct. 26 (4) (2004) 427–436, https://doi.org/10.1016/j.engstruct.2003.10.014.

[28] S.D. Akbas, Forced vibration analysis of functionally graded nanobeams, Int. J. Appl. Mech. 9 (7) (2017), https://doi.org/10.1142/S1758825117501009.

[29] T. Yan, J. Yang, Forced vibration of edge-cracked functionally graded beams due to a transverse moving load, Procedia Eng. 14 (2008) (2011) 3293–3300, https://doi.org/10.1016/j.proeng.2011.07.416.

[30] Ş.D. Akbaş, Bending of a cracked functionally graded nanobeam, Adv. Nano Res. 6 (3) (2018) 219–243, https://doi.org/10.12989/anr.2018.6.3.219.

[31] T. Van Lien, N.T. Duc, N.T. Khiem, Free vibration analysis of multiple cracked functionally graded timoshenko beams, Lat. Am. J. Solid. Struct. (2017) 1752–1766.

[32] S. Shabani, Y. Cunedioglu, Free vibration analysis of functionally graded beams with cracks, J. Appl. Comput. Mech. 6 (4) (2020) 908–919, https://doi.org/10.22055/JACM.2019.30065.1672.

[33] Ş.D. Akbaş, Forced vibration analysis of cracked nanobeams, J. Brazilian Soc. Mech. Sci. Eng. 40 (8) (2018) 39–55, https://doi.org/10.1007/s40430-018-1315-1.

[34] Ş.D. Akbaş, Free vibration characteristics of edge cracked functionally graded beams by using finite element method, Int. J. Eng. Trends Technol. 4 (10) (2013) 4590–4597.

[35] T. Van Lien, N.T. Duc, N.T. Khiem, A new form of frequency equation for functionally graded timoshenko beams with arbitrary number of open transverse cracks, Iran. J. Sci. Technol. - Trans. Mech. Eng. 43 (2009) (2019) 235–250, https://doi.org/10.1007/s40997-018-0152-2.

[36] T.E. Elaikh, O.O.O. Agboola, Investigation of transverse vibration characteristics of cracked axially moving functionally graded beam under thermal load, Trends Sci 19 (23) (2022), https://doi.org/10.48048/tis.2022.1349.

[37] O.O. Agboola, T.E. Elaikh, J.G. Oghonyon, O. Ibikunle, Effect of mass per unit length on freely vibrating simply supported Rayleigh beam, WSEAS Trans. Fluid Mech. 17 (October) (2022) 173–180, https://doi.org/10.37394/232013.2022.17.17.

[38] S.D. Akbaş, Wave propagation in edge cracked functionally graded beams under impact force, JVC/Journal Vib. Control 22 (10) (2016) 2443–2457, https://doi.org/10.1177/1077546314547531.

[39] M.Z. Nejad, A. Hadi, Non-local analysis of free vibration of bi-directional functionally graded Euler-Bernoulli nano-beams, Int. J. Eng. Sci. 105 (2016) 1–11, https://doi.org/10.1016/j.ijengsci.2016.04.011.

[40] K. Zhu, J. Chung, Vibration and stability analysis of a simply-supported Rayleigh beam with spinning and axial motions, Appl. Math. Model. 66 (2019) 362–382, https://doi.org/10.1016/j.apm.2018.09.021.

[41] N.A. Bachaya, T. Eh Elaikh, Transverse vibration of cracked graded Rayleigh beam with axial motion, Univ. Thi-Qar J. Eng. Sci. (2021), https://doi.org/10.31663/tqujes.11.2.390(2021).

[42] A. Shariati, D. won Jung, H. Mohammad-Sedighi, K.K. Żur, M. Habibi, M. Safa, Stability and dynamics of viscoelastic moving Rayleigh beams with an asymmetrical distribution of material parameters, Symmetry (Basel) 12 (4) (2020) 586, https://doi.org/10.3390/sym12040586.

[43] J. Fernández-Sáez, L. Rubio, C. Navarro, Approximate calculation of the fundamental frequency for bending vibrations of cracked beams, J. Sound Vib. 225 (2) (1999) 345–352, https://doi.org/10.1006/jsvi.1999.2251.

[44] L.F. Zhu, L.L. Ke, Y. Xiang, X.Q. Zhu, Y.S. Wang, Vibrational power flow analysis of cracked functionally graded beams, Thin-Walled Struct. 150 (July 2019) (2020), 106626, https://doi.org/10.1016/j.tws.2020.106626.

[45] T. Van Lien, N.T. Đuc, N.T. Khiem, Free and forced vibration analysis of multiple cracked fgm multi span continuous beams using dynamic stiffness method, Lat. Am. J. Solid. Struct. 16 (2) (2019), https://doi.org/10.1590/1679-78255242.

[46] A. Gee, S.M. Hashemi, Undamped free vibration analysis of functionally graded beams: a dynamic finite element approach, Appl. Mech. 3 (4) (2022) 1223–1239, https://doi.org/10.3390/applmech3040070.

[47] K.K. Pradhan, S. Chakraverty, S.K. Panigrahi, Implementation of numerical approximations in studying vibration of functionally graded beams, Int. J. Dyn. Control 6 (3) (2018) 1023–1046, https://doi.org/10.1007/s40435-017-0375-x.

[48] M. Şimşek, T. Kocatürk, Free and forced vibration of a functionally graded beam subjected to a concentrated moving harmonic load, Compos. Struct. 90 (4) (2009) 465–473, https://doi.org/10.1016/j.compstruct.2009.04.024.